Modulation of the Northern polar vortex by the Hunga Tonga-Hunga Ha'apai eruption and associated surface response

Ales Kuchar[1], Timofei Sukhodolov[2], Gabriel Chiodo[3,4], Andrin Jörimann[2,3], Jessica Kult-Herdin[1], Eugene Rozanov[2,5], and Harald H. Rieder[1]

[1]Institute of Meteorology and Climatology, BOKU University, Vienna, Austria
[2]Physikalisch-Meteorologisches Observatorium Davos/World Radiation Center (PMOD/WRC), Davos, Switzerland
[3]Institute for Atmospheric and Climate Science, ETH Zurich, Zurich, Switzerland
[4]Instituto de Geociencias (IGEO), CSIC-UCM, Madrid, Spain
[5]Ozone Layer and Upper Atmosphere Research Laboratory, Saint Petersburg State University, Russian Federation

Correspondence: A. Kuchar (ales.kuchar@boku.ac.at)

Abstract. The January 2022 Hunga Tonga-Hunga Ha'apai (HT) eruption injected sulfur dioxide and unprecedented amounts of water vapor (WV) into the stratosphere. Given the manifold impacts of previous volcanic eruptions, the full implications of these emissions are a topic of active research. This study explores the dynamical implications of the perturbed upper atmospheric composition using an ensemble simulation with the Earth System Model SOCOLv4. The simulations replicate the observed anomalies in the stratosphere and lower mesosphere's chemical composition and reveal a novel pathway linking water-rich volcanic eruptions to surface climate anomalies. We show that in early 2023 the excess WV caused significant negative anomalies in tropical upper-stratospheric/mesospheric ozone and temperature, forcing an atmospheric circulation response that particularly affects the Northern Hemisphere polar vortex (PV). The decreased temperature gradient leads to a weakening of the PV, which propagates downward similarly to sudden stratospheric warmings (SSWs) and drives surface anomalies via stratosphere-troposphere coupling. These results underscore the potential for HT to create favorable conditions for SSWs in subsequent winters as long as the near-stratopause cooling effect of excess WV persists. Our findings highlight the complex interactions between volcanic activity and climate dynamics and offer crucial insights for future climate modeling and attribution.

1 Introduction

The January 15, 2022 eruption of the Hunga Tonga-Hunga Ha'apai (HT) volcano was a unique and unprecedented event in the observational era. It released massive amounts of water vapor (WV), far exceeding previous records, and modest amount of sulfur dioxide (SO_2) into the stratosphere. This eruption injected between 140 and 150 Tg of WV and 0.4 Tg of SO_2 into the stratosphere, reaching mesosphere levels (Millán et al., 2022; Coy et al., 2022; Xu et al., 2022; Randel et al., 2023). The immediate and subsequent effects of the aerosol and WV plumes have been causing significant anomalies in atmospheric circulation, composition, and temperature (Coy et al., 2022; Yu et al., 2023; Wilmouth et al., 2023).

The radiative impacts of volcanic eruptions, particularly those associated with sulfate aerosols emerging following the SO_2 emissions, are well-known and have been widely studied (Robock, 2000; Marshall et al., 2022). The modulation of dynamical processes by volcanic eruptions and potential surface impacts, however, are incompletely understood. Typically, volcanic eruptions cause lower-stratospheric warming, which strengthens the polar vortex (PV) and may cause changes in stratosphere-troposphere coupling, resulting in surface warming over Eurasia and altered weather patterns across the NH (Stenchikov et al., 2002), although this connection has been recently questioned (Polvani et al., 2019; DallaSanta and Polvani, 2022). However, in the case of the HT eruption, this pronounced and canonical tropical lower stratospheric warming has not been observed, and its absence is most likely attributable to lower emissions of SO_2.

Instead, the HT eruption has led to significant anomalies in the stratospheric and lower-mesospheric ozone and temperature, which affected atmospheric circulation and particularly of the Southern Hemisphere (SH; Coy et al., 2022; Wang et al., 2023; Yu et al., 2023; Zhang et al., 2024a). The increased OH concentrations induced by the excess WV from the HT eruption led to ozone depletion and temperature anomalies in the upper stratosphere and lower mesosphere (Santee et al., 2023; Fleming et al., 2024).

The excess of WV due to the HT eruption exerts a forcing around the tropical stratopause. Studies on the influence of solar variability (Gray et al., 2010; Kuchar et al., 2015; Mitchell et al., 2015) suggest that such forcing at the stratopause level can also act as a significant modulator of atmospheric dynamics. This raises two main questions: 1) Do similar modulation effects emerge for the HT eruption? and 2) if so, do changes in the tropospheric circulation emerge in response to the increase in WV, similarly to those emerging for uniformly doubling WV in the lower stratosphere (Joshi et al., 2006; Maycock et al., 2013)?

This study explores a novel pathway by which the HT eruption may have modulated stratospheric and mesospheric conditions and consequently impacted surface climate. Here we use a set of ensemble sensitivity simulations performed with the Earth System model (ESM) SOCOLv4 with and without the HT forcing to analyze the effects of the HT eruption and validate these simulations with observational data for H_2O and aerosol and discuss other variables using available studies (see Section A1 in Appendix). We then assess the statistical significance of the detected effects and examine the mechanisms through which the HT eruption could influence the stratospheric PV in 2023 or 2024, creating more favorable conditions for the onset of sudden stratospheric warming (SSW). Both winter seasons have been accompanied by record amounts of Rossby waves propagating upward from the troposphere (Vargin et al., 2024; Newman et al., 2024). Finally, we conclude with a summary of the results, a discussion on the general forcing mechanism in the following winters when the HT forcing would persist and an outlook of how these dynamically-induced events could be further explored.

2 Results

We set the scene by illustrating the evolution of the monthly and zonal-mean structure of water vapor, ozone, OH and temperature for the extended winter 2022/2023 in Fig. 1. About ten months after the eruption, the WV inputs of HT have distributed across the middle and upper stratosphere and the mesosphere. In December 2022, the WV plume (panel **A**) is mostly localized around 20 hPa and 45°S, but has already started to disperse into the NH and beyond the stratopause. This distributed HT WV anomaly affects ozone globally, as evidenced by the negative anomalies in the lower mesosphere and positive anomalies in the mid-stratosphere (panel **F**). The positive O_3 anomaly can be attributed to increased conversion of NO_x to the HNO_3 reservoir (see Fig. A5) due to higher abundance of OH (Fleming et al., 2024) as shown in Fig. 1, as well as due to hydrolysis of N_2O_5 on aerosol surfaces (Kinnison et al., 1994). Under elevated aerosol loading (see Fig. A2) the heterogeneous reactions serve as a significant source of chlorine activation and ozone loss in the lower stratosphere, which may include reaction of HCl with HOBr (Zhang et al., 2024b; Evan et al., 2023), with HOBr being the product of $BrONO_2$ hydrolysis (see Fig. A6). In the lower mesosphere, the negative ozone anomaly is a direct consequence of the chemical pathway initiated by the excess of OH. Note, the significant OH anomalies, similar to those of O_3 and H_2O, at that time do not reach the Northern polar cap. Radiatively-induced anomalies in temperature emerge in our simulations around and above the stratopause mainly as consequence of the reduced absorption of ultraviolet radiation by ozone (see Fig. 4.24 in Brasseur and Solomon, 2005) as also reported by recent modeling studies (Fleming et al., 2024; Randel et al., 2024).

The negative mesospheric temperature anomaly emerges at the beginning of boreal winter and extends up to 20°N latitude (see Fig. 1**P–T**). The subsequent temporal evolution and propagation towards high latitudes we discuss further below. To illustrate the latitudinal variations, anomalies and impacts in detail, we plot in Fig.2 the evolution of daily temperature profiles during the months JFMAM in 2023 for northern equatorial latitudes (0°–20°N; **A**) and the northern polar cap (60°–90°N; **B**). Here it becomes obvious that the negative mesospheric temperature anomaly persisted at lower latitudes through the whole winter 2022/2023 (see Fig. 2**A**). This is in agreement with the observational estimates from satellites (Fleming et al., 2024) and GPS radio occultation (Veenus and Das, 2023; Stocker et al., 2024). In contrast, at higher latitudes no significant persistent mesospheric temperature anomaly is found (see Fig. 2**B**). This difference between low and high latitudes results in a reduced meridional temperature gradient in the upper stratosphere and the lower mesosphere, which via thermal wind relation, weakens the polar-night jet.

In consequence, the weakened winds allow more planetary waves (PW) to propagate upward into the stratosphere (Charney and Drazin, 1961), where they break and dissipate and thereby further weaken the already disturbed stratospheric PV. The slowdown of the winds and the associated increase in polar temperature (see Fig. 2**B**) emerges in our simulations as early as February but is fully evident in March 2023. The stratospheric polar warming connected with the enhanced Brewer-Dobson circulation is directly coupled to the cooling aloft and associated weaker meridional circulation. Furthermore, along with the temperature change, we detected (subsequently) increasing concentrations of ozone over the polar cap in March and April ((see Fig. 1**I–J** or Fig. 13 in Fleming et al., 2024). The temperature structure across the upper atmosphere displayed in Fig. 2 resembles the transition from a more positive to a more negative phase of the Northern Annual Mode (NAM; see Section A3) in the stratosphere and lower mesosphere, respectively. Figure 2**C** illustrates how the HT forcing projects on NAM (shading). Along with NAM we provide the eddy heat flux (EHF; green line) at 100 hPa as a proxy for upward propagation of planetary waves (e.g., Newman et al., 2001). The downward phase propagation of negative NAM anomalies illustrates the role of wave mean-flow interactions (Baldwin and Dunkerton, 2001), as also indicated by Eliassen-Palm flux diagnostics (see Fig. A7). Since the EHF response lags slightly behind the NAM, the triggering mechanism appears to be similar to SSWs, and how

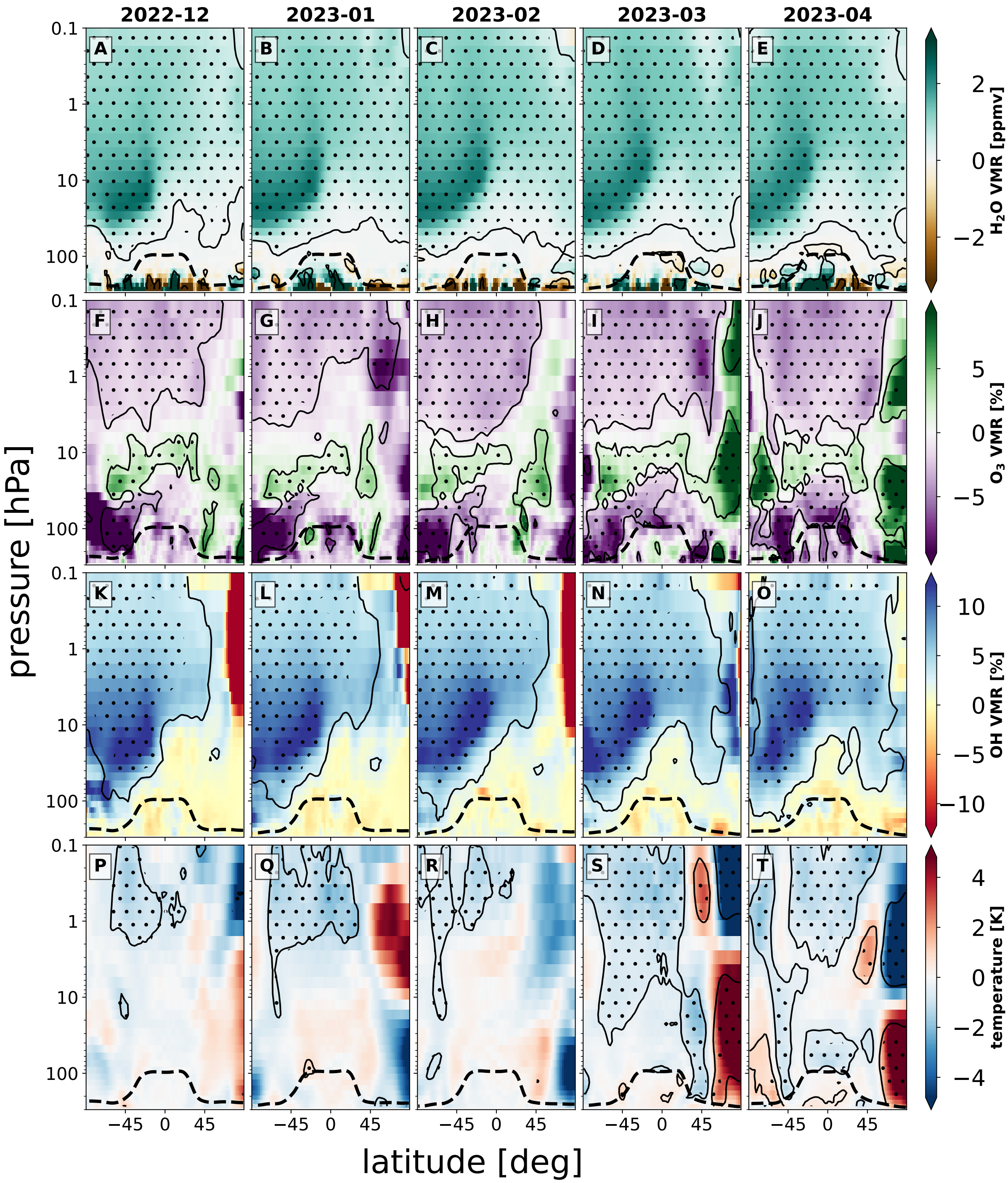

Figure 1. Monthly zonal-mean structure of water vapor volume mixing ratio (VMR; first row **A**–**E** in ppmv), ozone (second row **F**–**J** in %), OH (third row **K**–**O** in %) and temperature (fourth row **P**–**T** in K) anomalies, respectively, for the extended boreal winter 2022/2023. Anomalies are expressed as difference between the SOCOLv4 simulation with and without the HT forcing. 2σ statistical significance from t-test is indicated by dots. 1σ FDR correction (see Section A2) is indicated by black solid contour lines. Tropopause pressure level is visualized by black dashed line.

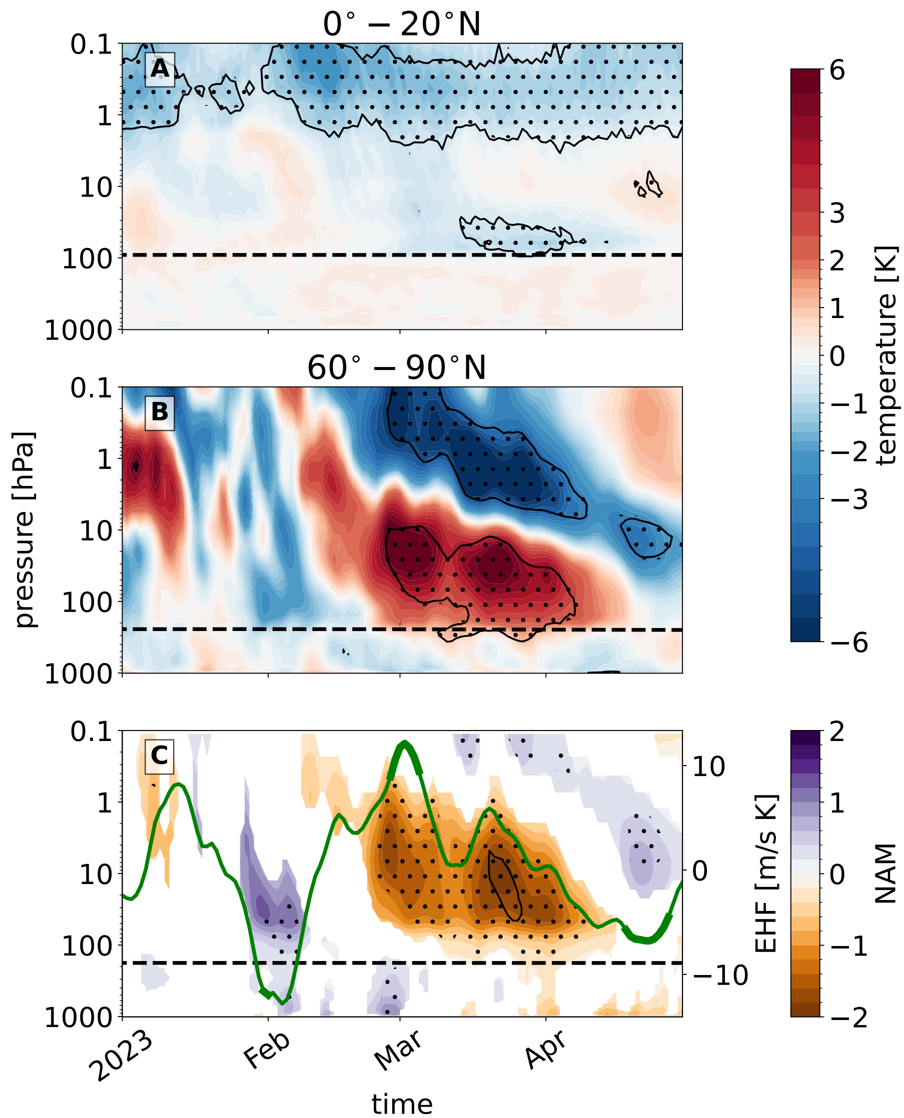

Figure 2. Weighted zonally-averaged temperature averaged over 0°–20°N (**A**) and 60°–90°N (**B**), and Northern Annual Mode (NAM; shading in **C**) and Eddy Heat Flux at 100 hPa averaged over 45°–75°N (EHF in $\mathrm{m/s\,K}$; green line in **C**) daily anomalies for the months JFMA in 2023. Anomalies are expressed as difference between the SOCOLv4 simulation with and without the HT forcing. 2σ statistical significance from t-test is indicated by dots. 1σ FDR correction (see Section A2) is indicated by black solid contour lines. To highlight the signal propagation, we mask out non-significant NAM values at 1σ.

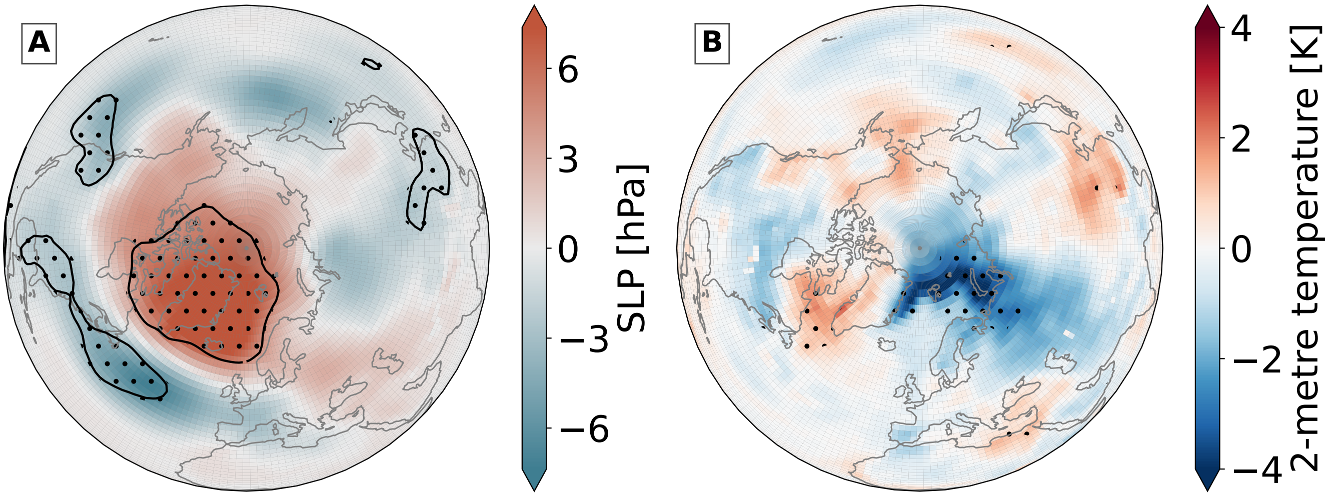

Figure 3. Monthly anomaly of Sea level pressure (**A**; SLP in hPa) and surface air temperature (**B**; in K) in April 2023. Anomalies are expressed as difference between the SOCOLv4 simulation with and without the HT forcing. 2σ statistical significance from t-test is indicated by dots. 1σ FDR correction (see Section A2) is indicated by black solid contour lines.

dynamically-forced anomalies in the upper stratosphere and lower mesosphere may be communicated downward and thus control PWs (Hitchcock and Haynes, 2016).

Turning the focus to lower levels, it becomes apparent that negative NAM anomalies emerge close to the surface ($\sim 1000\,\mathrm{hPa}$) in April, which follow the significant negative NAM anomalies in the stratosphere in the preceding months. This time lag suggests that stratospheric anomalies are triggering some of the changes observed in the troposphere (Thompson et al., 2005). Geopotential height anomalies (see Fig. A8) again support a downward propagation of the signal from the stratosphere all the way to surface. To further explore these conditions, we turn the focus to the analysis of the monthly sea level pressure (SLP in hPa) anomaly in April 2023, which is shown in Fig. 3. Here we identify a positive SLP anomaly in polar and negative SLP anomaly in mid-latitudes. This pattern is characteristic of a weaker stratospheric PV, and is associated with an equatorward shift of the tropospheric jet stream. The canonical temperature pattern with a pronounced cold anomaly in Northern Europe (see Fig. 3**B**) clearly arises for this weak vortex event (Domeisen and Butler, 2020; Kolstad et al., 2022). Generally, the coupling is independent of the forcing mechanism causing these changes in PV and is present across all timescales (Kidston et al., 2015).

3 Discussion and summary

The January 2022 Hunga Tonga-Hunga Ha'apai volcanic eruption significantly modified the radiative balance, photochemistry, and dynamics of the stratosphere and lower mesosphere, as has been extensively documented (Coy et al., 2022; Sellitto et al., 2022; Jenkins et al., 2023; Santee et al., 2023). Here we add to the discussion of HT effects by illustrating for the first time the dynamical stratosphere-troposphere-surface coupling in the NH following the eruption. We show in a series of ESM sensitivity simulations how the WV input propagated upward and poleward, and thereby impacted the stratospheric PV and contributed to the emergence of SSW in boreal winter 2022/2023 and subsequent surface SLP anomalies. Similarly, the HT eruption induced a marked warming anomaly in the Arctic region, with temperatures rising by up to 2 K near the North Pole in early 2022 (Bao et al., 2023).

Our results thereby illustrate how anomalies in OH, nitrogen species, and O_3, induced in the stratosphere and lower mesosphere due to excess of WV after the HT eruption, influence upper atmosphere dynamics via alteration of temperature gradients, and thereby lead to the emergence of a negative NAM anomaly at upper levels during the winter-spring transition that manifests by April 2023 in SLP. We begin our attribution in the upper stratosphere and lower mesosphere, where increased OH concentrations induce a negative ozone anomaly. In consequence, our set of sensitivity simulations illustrates a radiatively-induced negative temperature response in equatorial latitudes up to 20°N latitude, which leads to a reduced horizontal hemispheric temperature gradient. This alteration of the temperature gradient is associated with weaker winds via the thermal wind relation. As weaker winds emerge in the stratosphere (negative NAM anomaly) we find that the anomaly propagates with time downward illustrating the role of wave mean-flow interactions, similarly as during SSWs. This mechanism provides in summary a chain of processes which could have contributed to the observed SSW during the winter 2022/2023. We note that the causal link in observations cannot be entirely established on the one hand due to internal stratospheric variability driving SSWs (Baldwin et al., 2021) and on the other the free-running ocean set up of our simulations. However, all things equal our results clearly show that HT has provided favorable conditions for the emergence of late winter NH SSWs in 2023.

Two major SSWs have been detected during the extended winter 2023/2024 (see Fig. A9). Our model-projected forcing during that winter was weaker due to a quicker WV dissipation from the stratosphere (see Fig. A4). Thus, we do not detect any significant dynamical responses. While Randel et al. (2024) observed the strong ($\sim -2\,\mathrm{K}$) lower-mesospheric cooling after middle 2023, the mechanism suggested and simulated by SOCOLv4 above should be valid for the winter 2024 and following winters if the lower-mesospheric cooling would be persistent and strong enough due to the excess of WV. This mechanism establishes a novel pathway how water-rich volcanic eruptions can indirectly impact the surface climate via downward propagation of the dynamical perturbation from the stratosphere and lower mesosphere. Thereby it adds to the manifestations of stratosphere-troposphere coupling on various timescales.

Future work should vet the proposed mechanism, ideally within multi-model inter-comparison projects (Zhu et al., 2024), and explore whether the HT forcing also contributed to the disruption of the stratospheric PV during the following winters. Given the interhemispheric extent of cooling in the upper stratosphere and lower mesosphere, which could similarly affect the persistence of PV in the SH, future studies could explore the PV response in the SH and its coupling with the troposphere. Furthermore, the stratospheric response could be impacted by the phase of the quasi-biennial oscillation as recently suggested by Jucker et al. (2024).

Code and data availability. SWOOSHv2.7 data can be downloaded from https://csl.noaa.gov/groups/csl8/swoosh/. The MERRA2 reanalysis dataset provided by Martineau (2022) referred as the Reanalysis Intercomparison Dataset (RID) can be downloaded from https:

//www.jamstec.go.jp/ridinfo/. M2-SCREAM can be downloaded from https://acdisc.gesdisc.eosdis.nasa.gov/opendap/hyrax/M2SCREAM/GMAO_M2SCREAM_INST3_CHEM.1/. GloSSAC data can be downloaded from https://asdc.larc.nasa.gov/project/GloSSAC. The code that was used to produce all plots in this study is available via Zenodo (Kuchar, 2025b). Any direct access to full simulation data can be arranged by contacting the authors. All postprocessed data files for this study are provided via Mendeley Data (Kuchar, 2025a).

Appendix A: Methods

A1 SOCOLv4 simulations

We use a set of ensemble sensitivity simulations performed with the Earth System model SOCOLv4 (Sukhodolov et al., 2021), which comprises comprehensive stratospheric chemistry and sulfate aerosol microphysics, to assess the impacts of the HT eruption on stratospheric composition and dynamics. SOCOLv4 is used in a T63 horizontal resolution ($1.9° \times 1.9°$) and a vertical resolution of 47 vertical levels (till $\sim$0.01 hPa), with the boundary conditions following the recommendations of the Model Intercomparison Project Phase 6 (CMIP6; Eyring et al., 2016). The quasi-biennial oscillation (QBO) is not self-generated with the employed vertical resolution, and therefore it is nudged in the model. Since the simulations expand into the future, instead of the actual QBO observational data we used the same data but shifted back by 16 years, allowing to keep a QBO phase during the eruption that is consistent with observations. The SOCOLv4 model is widely used for process analyses in stratospheric research and has contributed to the recent Chemistry-Climate Model Initiative (CCMI; Morgenstern et al., 2022; Friedel et al., 2023) and interactive stratospheric aerosol model intercomparison (ISA-MIP: Quaglia et al., 2023; Brodowsky et al., 2024) among others.

Our set of simulations comprises an ensemble of transient simulations with and without HT forcing. We perform a 5-year spin-up prior to the HT eruption, so that by the date of the event each ensemble member has a different ocean state, contributing to internal variability in the ensemble. In January 2022 we then branch out two ensembles, one with and one without the HT forcing. Both ensembles comprise 10 ensemble members. Note that the WV freezing around the emission region (22°S—14°S; 182°E-–186°E and 25–30 km within January 15) was turned off for several days to avoid artifacts and mimic the estimated magnitude ($\sim 150\,\mathrm{Tg}$) of the WV forcing by Millán et al. (2022) and M2-SCREAM (see Fig. A1**A**; Wargan et al., 2023). Another way to avoid freezing artifacts would be to broaden the emission region vertically. The M2-SCREAM WV anomaly is within the ensemble spread; however, this spread is quite wide, suggesting that the WV plume evolution could have been strongly modulated by the background dynamical conditions. In addition, the modeled WV anomaly shows a more pronounced seasonal cycle.

According to the fitted decay, we project the stratospheric WV burden to represent an enhanced forcing over the next years and only return to pre-HT background values by 2031. The excess of stratospheric WV returns to the troposphere by sedimentation of PSCs within the SH PV, and is transported to higher latitudes of both hemispheres via the Brewer-Dobson circulation (BDC). The combination of these processes leads to an exponential decay of the WV burden with an estimated e-folding time of $\sim$2.5 years based on the fitted period of 2023–2025 (see Fig. A1**B**). Our decay estimate is in agreement with

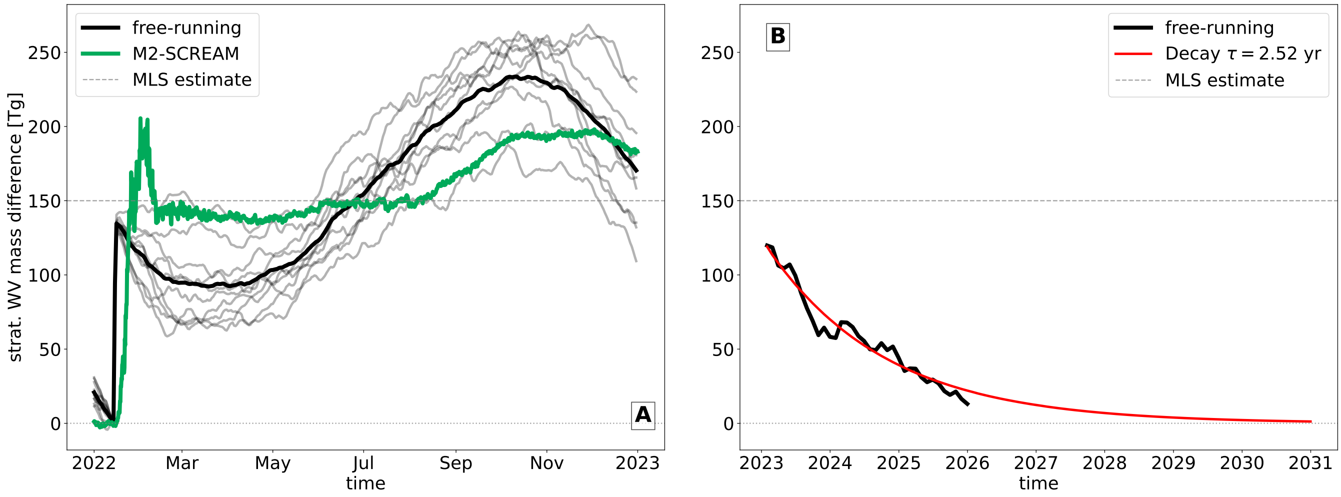

Figure A1. (A) Globally averaged daily anomaly of integrated stratospheric water vapor during January 2022 for the free-running (black line) SOCOLv4 simulations and M2-SCREAM (green line) with respect to January 14, 2022. **(B)** Monthly anomaly of integrated stratospheric water vapor for the free-running SOCOLv4 simulations (black line) for the period 2023-2025 and the corresponding fitted decay (red line) with e-folding time τ of 2.52 years. Horizontal dotted line represent the estimated magnitude after the HT eruption by Millán et al. (2022).

Fleming et al. (2024), who used a free-running 2D model, but about half of the estimate provided by Zhou et al. (2024), who estimated an e-folding time scale of 4 years using a chemical transport model with the perpetual ERA5 meteorology.

Furthermore, we use data from SWOOSH for daily H_2O (Davis et al., 2016) and GloSSAC for monthly mean Surface Area Density (SAD; NASA/LARC/SD/ASDC, 2023) to validate the SOCOLv4 anomalies (see Fig. A2 vs. A3). Note, we retrieve SAD fields using extinction coefficients on all 4 GloSSAC wavelengths, according to the SAGE-4λ method (Jörimann, 2025-01-14). The SAD background in GloSSAC is a bit higher in higher latitudes compared to SOCOLv4, since for GloSSAC we used the 1999-2004 climatology representative for the volcanically quiescent conditions, while for SOCOLv4 we used the difference between experiments with and without HT. The aerosol plume evolves in a similar spatio-temporal manner, i.e. towards the SH and lower pressure levels. The WV plume extends horizontally, firstly towards the SH PV and then across the equator according to climatology of the residual circulation. During the boreal winter 2023, the WV anomaly is spread across all latitudes from middle stratosphere upward in both SWOOSH and SOCOLv4. The reduction of water in SOCOLv4 starts to be apparent in the end of 2023 in contrast to SWOOSH where the WV anomaly sustains its values. Globally averaged stratospheric and lower-mesospheric water vapour in Fig. A4 indicates a slight deficiency of SOCOLv4 as the anomalous water dissipates faster as seen in observations (e.g. MLS) or occuring in other models (cf. with WACCM in Figs. 1, 2 and 3 in Randel et al., 2024). Note that our experiment protocol differs to WACCM and other models (Zhu et al., 2024), which were either nudged to reanalysis or initialized from the observed sea-surface temperatures.

The too-strong tropical-to-midlatitude mixing and too-fast tropical ascent is a common peculiarity for chemistry–climate models (Dietmüller et al., 2018). As it has been already reported (Sukhodolov et al., 2021), it could be addressed in future

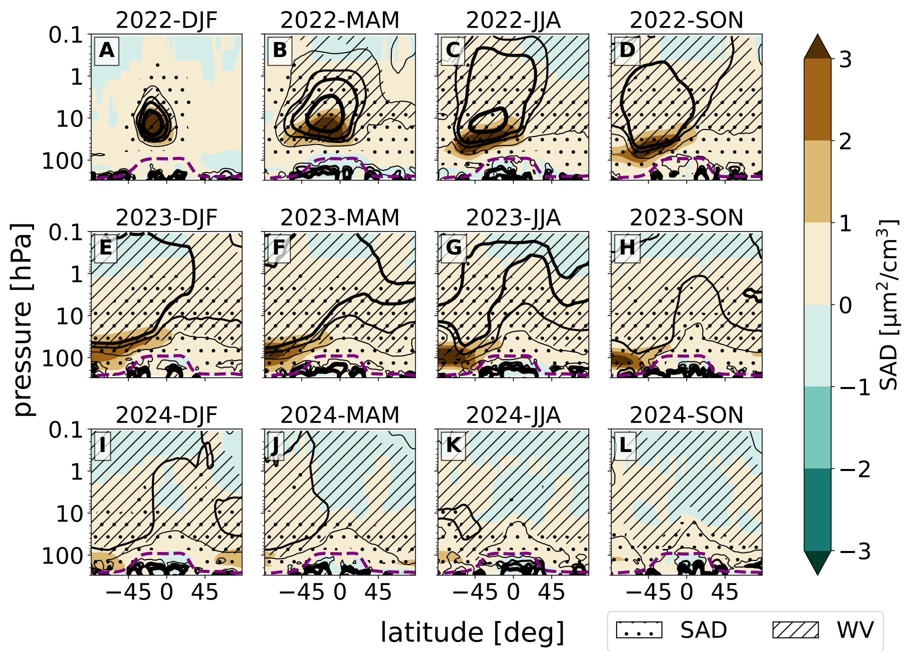

Figure A2. Seasonal zonal-mean structure of Surface Area Density (SAD; shading in $\mu\mathrm{m}^2/\mathrm{cm}^3$) and Water Vapour (WV; solid contour lines: $0.1, 0.5, 1, 3\,\mathrm{ppmv}$) volume mixing ratio. Anomalies are expressed as difference between the SOCOLv4 simulation with and without the HT forcing. 2σ statistical significance from t-test is indicated by dots and hatching in case of SAD and WV, respectively. Tropopause pressure level is visualized by purple dashed lines

simulations with higher vertical resolution (Brodowsky et al., 2021). Nevertheless, during late 2022 and early 2023 the model is in a good agreement with observations in terms of the WV and aerosol forcing.

A2 Calculation of anomalies

Throughout our analysis we evaluate significance fields using the minimum local p-values from Student's t-test with global test statistics using the False Detection Rate (FDR) methodology (Wilks, 2006), first described by Benjamini and Hochberg (1995) and later promoted by Wilks (2016) in the atmospheric sciences. All illustrations in Section 2 show differences between simulations with and without HT forcing. For significance regions we show in addition to the dots indicating local p-values < 0.05, boundaries of p-values < 0.32 corrected for FDR.

A3 Calculation of Northern Annual Mode

The Northern Annular Mode (NAM) was calculated at each pressure level as the first Empirical Orthogonal Function (EOF) of the daily, latitude weighted, zonal mean zonal wind poleward of the NH (Gerber et al., 2008). The NAM index was defined as the Principal Component time series associated with the first EOF and standardized. Positive and negative NAM values

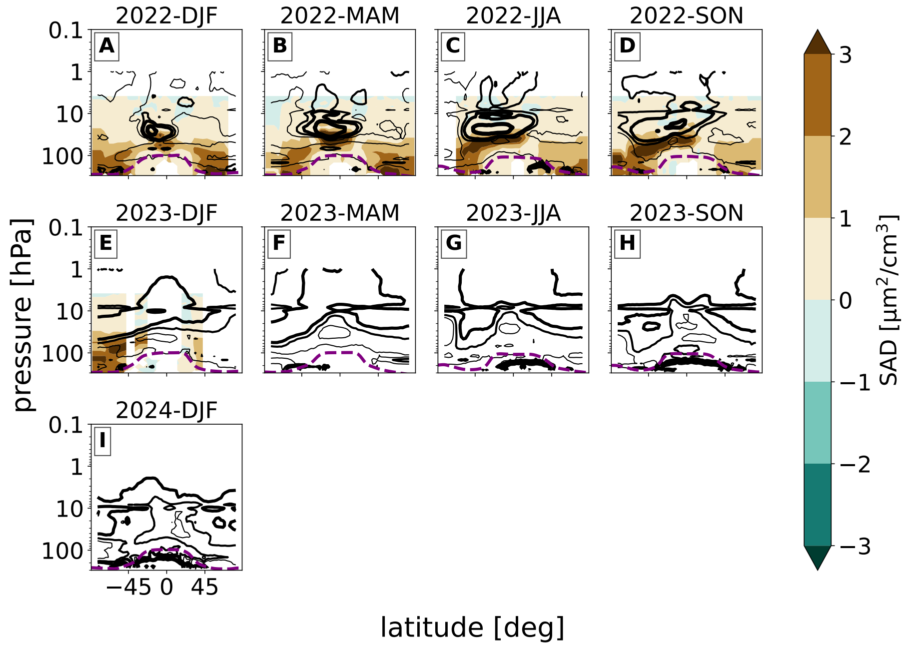

Figure A3. Seasonal zonal-mean structure of Surface Area Density (SAD; shading in $\mu\mathrm{m}^2/\mathrm{cm}^3$) and Water Vapour (WV; solid contour lines: $0.1, 0.5, 1, 3\,\mathrm{mol/mol}$) volume mixing ratio. SAD and WV anomalies in GloSSAC and SWOOSH are expressed as difference with respect to climatology for the period 1999–2004 and 1984–2023, respectively. Tropopause pressure level is visualized by purple dashed line

correspond to strong and weak PV events, respectively, with different thresholds used for the SSW identification (Baldwin and Dunkerton, 2001; Gerber and Polvani, 2009; Jucker, 2016).

A4 Eliassen-Palm flux diagnostics

The response of resolved waves is investigated using the Eliassen-Palm flux diagnostics (EPF; Andrews and McIntyre, 1987). EP fluxes are computed and scaled following Jucker (2021). The EPF convergence serves as an indicator of wave dissipation and the EPF divergence (EPFD) indicates sourcing.

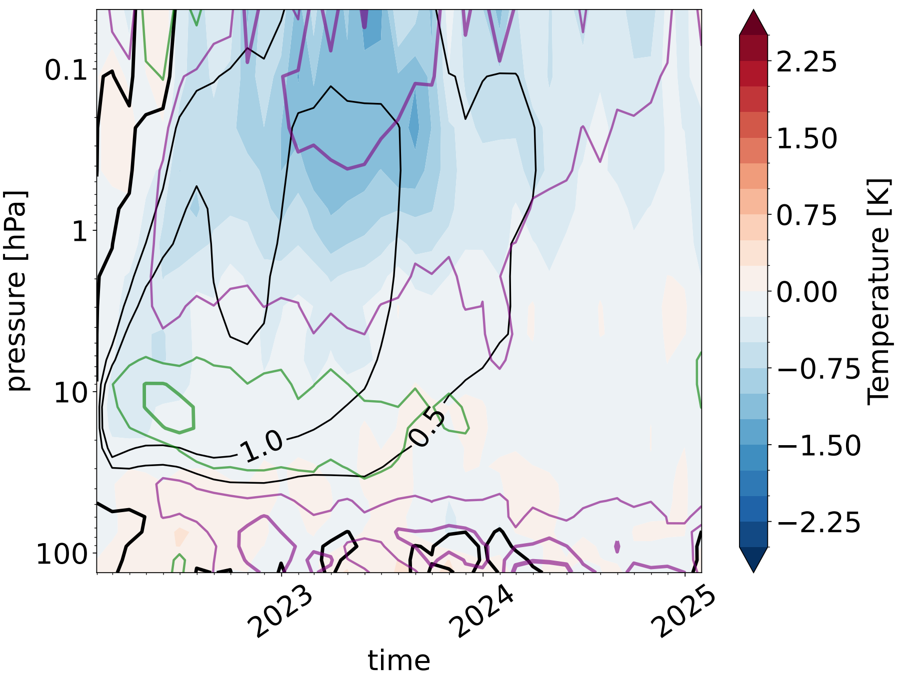

Figure A4. Monthly global-mean evolution of temperature (shading in K), water vapour volume mixing ratio (black solid contour lines: $\mathbf{0}, 0.5, 1, 3\,\mathrm{ppmv}$) and ozone volume mixing ratio (in %; purple solid contour lines: $-5, -3, -1$; green solid contour lines: $1, 3, 5$) between 100 and $0.01\,\mathrm{hPa}$. Anomalies are expressed as difference between the SOCOLv4 simulation with and without the HT forcing.

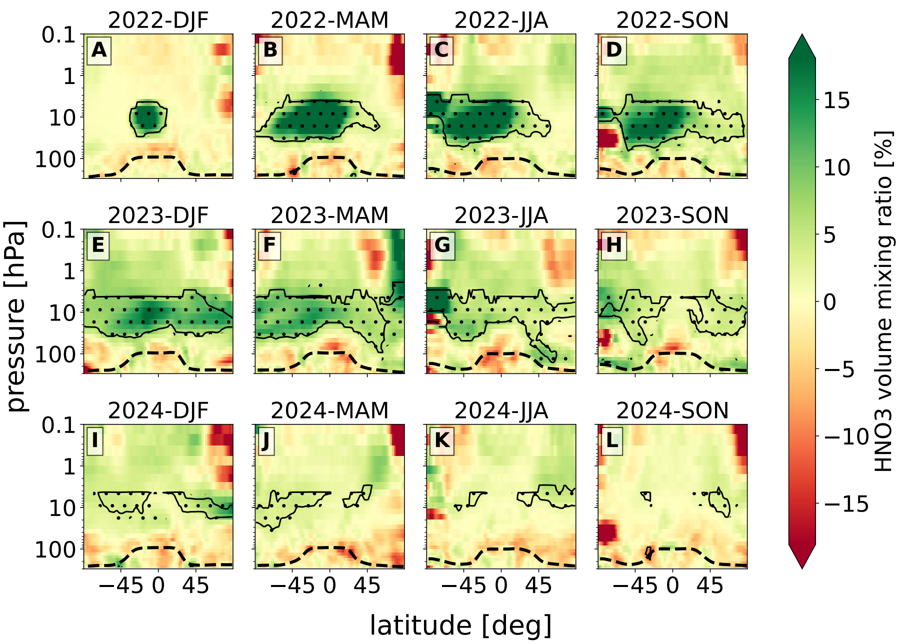

Figure A5. Seasonal zonal-mean structure of HNO_3 volume mixing ratio (**A**–**L** in %). Anomalies are expressed as difference between the SOCOLv4 simulation with and without the HT forcing. 2σ statistical significance from t-test is indicated by dots. 1σ FDR correction (see Section A2) is indicated by black solid contour lines. Tropopause pressure level is visualized by black dashed line

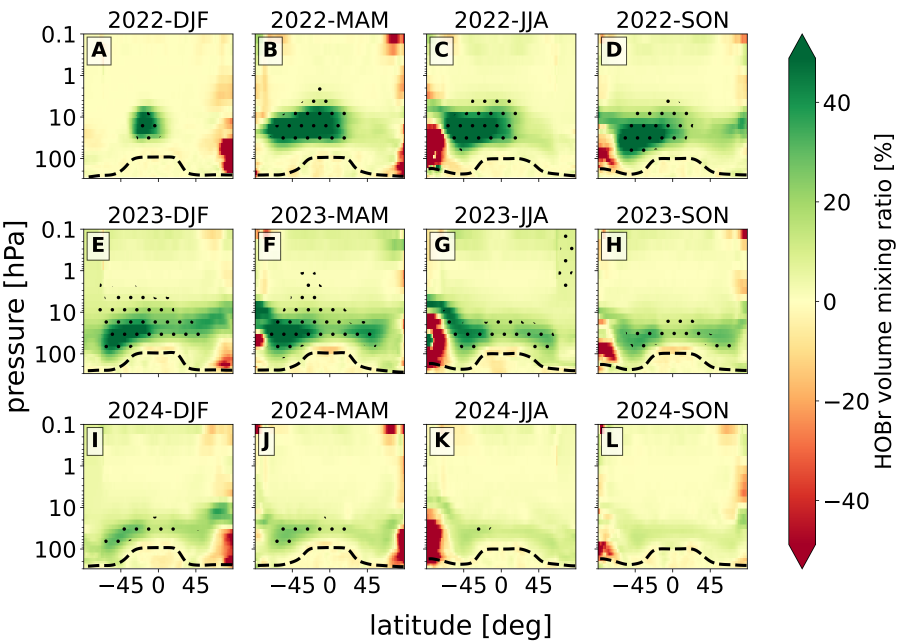

Figure A6. Seasonal zonal-mean structure of HOBr volume mixing ratio (**A**–**L** in %). Anomalies are expressed as difference between the SOCOLv4 simulation with and without the HT forcing. 2σ statistical significance from t-test is indicated by dots. 1σ FDR correction (see Section A2) is indicated by black solid contour lines. Tropopause pressure level is visualized by black dashed line

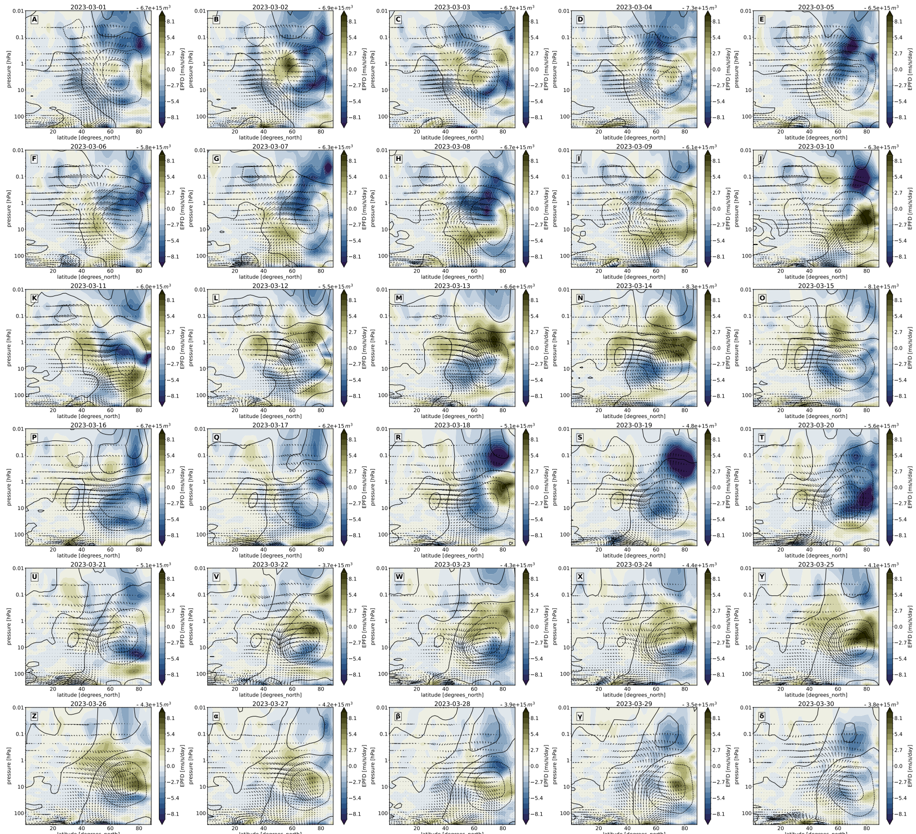

Figure A7. Daily anomalies of the Eliassen-Palm flux (EPF; arrows; in $(\mathrm{m}^2/\mathrm{s}^2; \mathrm{hPa\,m}/\mathrm{s}^2)$) and its divergence (EPFD; shading; in $\mathrm{m\,s}^{-1}\,\mathrm{day}^{-1}$) and zonal mean zonal wind (solid (positive) and dashed (negative) contours; in $\mathrm{m/s}$) in March 2023.

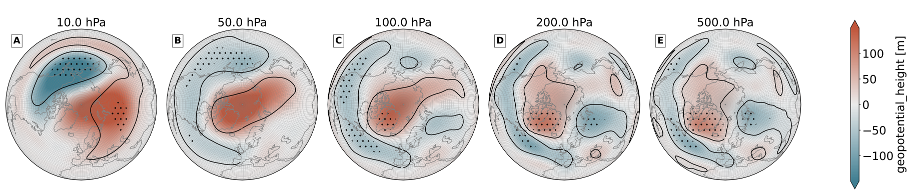

Figure A8. Monthly geopotential height anomalies (shading; m) at 10, 50, 100, 200 and 500 hPa in April 2023. 2σ statistical significance from t-test is indicated by dots. 1σ FDR correction (see Section A2) is indicated by black solid contour lines.

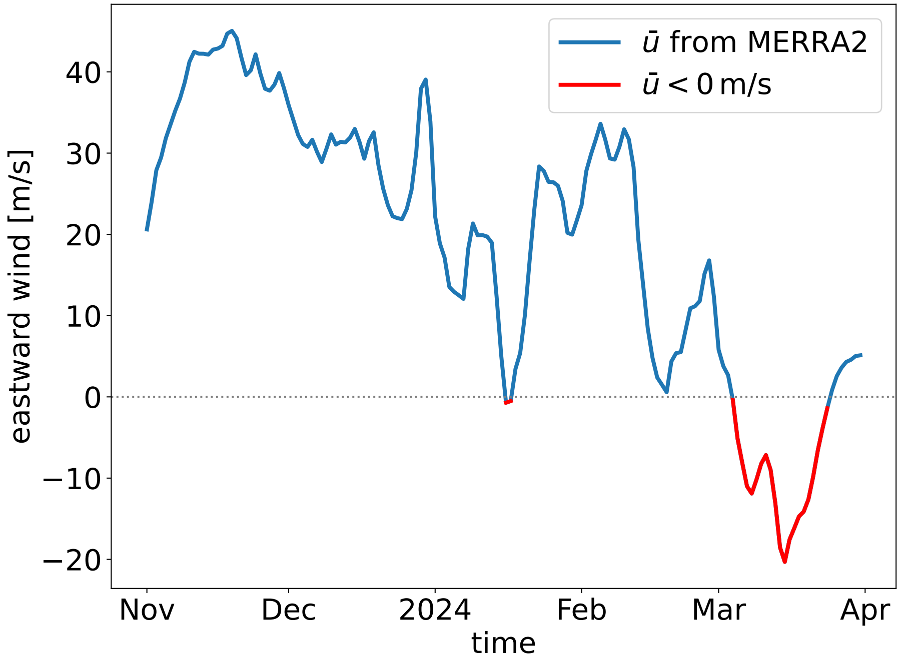

Figure A9. Daily zonal-mean zonal wind at 10 hPa and 60°N based on the MERRA2 dataset (Gelaro et al., 2017). It documents two major SSWs in the 2023/2024 winter.

Author contributions. AK and TS designed the study. TS set up and carried out the model simulations. AK analysed the data. AK, TS and AJ curated the data. AK compiled the manuscript with inputs of all other authors.

Competing interests. The authors declare that they have no conflict of interest.

Acknowledgements. AK and HR acknowledge support by the BOKU University. TS and AJ acknowledge support from the Swiss National Science Foundation (SNSF) project AEON (grant no. 200020E_219166). TS also acknowledges support from Karbacher Fonds, Graubünden, Switzerland. ER was partly supported by Saint-Petersburg State University (research grant 116234986). Simulations have been performed at the ETH cluster EULER and Swiss National Supercomputing Centre (CSCS) under project s1191. GC acknowledges support by the European Commission within the ERC Starting Grant N. 101078127.

References

Andrews, D. G. and McIntyre, M. E.: JR Holton, and CB Leovy, 1987: Middle Atmosphere Dynamics, 1987.

Baldwin, M. P. and Dunkerton, T. J.: Stratospheric Harbingers of Anomalous Weather Regimes, Science, 294, 581–584, https://doi.org/10.1126/science.1063315, 2001.

Baldwin, M. P., Ayarzagüena, B., Birner, T., Butchart, N., Butler, A. H., Charlton-Perez, A. J., Domeisen, D. I. V., Garfinkel, C. I., Garny, H., Gerber, E. P., Hegglin, M. I., Langematz, U., and Pedatella, N. M.: Sudden Stratospheric Warmings, Reviews of Geophysics, 59, e2020RG000 708, https://doi.org/https://doi.org/10.1029/2020RG000708, e2020RG000708 10.1029/2020RG000708, 2021.

Bao, Y., Song, Y., Shu, Q., He, Y., and Qiao, F.: Tonga volcanic eruption triggered anomalous Arctic warming in early 2022, Ocean Modelling, 186, 102 258, 2023.

Benjamini, Y. and Hochberg, Y.: Controlling the false discovery rate: A practical and powerful approach to multiple testing, J. Roy. Stat. Soc., 57B, 289–300, 1995.

Brasseur, G. P. and Solomon, S.: Aeronomy of the middle atmosphere: Chemistry and physics of the stratosphere and mesosphere, vol. 32, Springer Science & Business Media, 2005.

Brodowsky, C., Sukhodolov, T., Feinberg, A., Höpfner, M., Peter, T., Stenke, A., and Rozanov, E.: Modeling the Sulfate Aerosol Evolution After Recent Moderate Volcanic Activity, 2008–2012, Journal of Geophysical Research: Atmospheres, 126, e2021JD035 472, https://doi.org/https://doi.org/10.1029/2021JD035472, e2021JD035472 2021JD035472, 2021.

Brodowsky, C. V., Sukhodolov, T., Chiodo, G., Aquila, V., Bekki, S., Dhomse, S. S., Höpfner, M., Laakso, A., Mann, G. W., Niemeier, U., Pitari, G., Quaglia, I., Rozanov, E., Schmidt, A., Sekiya, T., Tilmes, S., Timmreck, C., Vattioni, S., Visioni, D., Yu, P., Zhu, Y., and Peter, T.: Analysis of the global atmospheric background sulfur budget in a multi-model framework, Atmospheric Chemistry and Physics, 24, 5513–5548, https://doi.org/10.5194/acp-24-5513-2024, 2024.

Charney, J. G. and Drazin, P. G.: Propagation of planetary-scale disturbances from the lower into the upper atmosphere, Journal of Geophysical Research, 66, 83–109, 1961.

Coy, L., Newman, P. A., Wargan, K., Partyka, G., Strahan, S. E., and Pawson, S.: Stratospheric Circulation Changes Associated With the Hunga Tonga-Hunga Ha'apai Eruption, Geophysical Research Letters, 49, e2022GL100 982, https://doi.org/https://doi.org/10.1029/2022GL100982, e2022GL100982 2022GL100982, 2022.

DallaSanta, K. and Polvani, L. M.: Volcanic stratospheric injections up to 160 Tg(S) yield a Eurasian winter warming indistinguishable from internal variability, Atmospheric Chemistry and Physics, 22, 8843–8862, https://doi.org/10.5194/acp-22-8843-2022, 2022.

Davis, S. M., Rosenlof, K. H., Hassler, B., Hurst, D. F., Read, W. G., Vömel, H., Selkirk, H., Fujiwara, M., and Damadeo, R.: The Stratospheric Water and Ozone Satellite Homogenized (SWOOSH) database: a long-term database for climate studies, Earth System Science Data, 8, 461–490, https://doi.org/10.5194/essd-8-461-2016, 2016.

Dietmüller, S., Eichinger, R., Garny, H., Birner, T., Boenisch, H., Pitari, G., Mancini, E., Visioni, D., Stenke, A., Revell, L., Rozanov, E., Plummer, D. A., Scinocca, J., Jöckel, P., Oman, L., Deushi, M., Kiyotaka, S., Kinnison, D. E., Garcia, R., Morgenstern, O., Zeng, G., Stone, K. A., and Schofield, R.: Quantifying the effect of mixing on the mean age of air in CCMVal-2 and CCMI-1 models, Atmospheric Chemistry and Physics, 18, 6699–6720, https://doi.org/10.5194/acp-18-6699-2018, 2018.

Domeisen, D. I. and Butler, A. H.: Stratospheric drivers of extreme events at the Earth's surface, Communications Earth & Environment, 1, 59, https://doi.org/10.1038/s43247-020-00060-z, 2020.

Evan, S., Brioude, J., Rosenlof, K. H., Gao, R.-S., Portmann, R. W., Zhu, Y., Volkamer, R., Lee, C. F., Metzger, J.-M., Lamy, K., et al.: Rapid ozone depletion after humidification of the stratosphere by the Hunga Tonga Eruption, Science, 382, eadg2551, 2023.

Eyring, V., Bony, S., Meehl, G. A., Senior, C. A., Stevens, B., Stouffer, R. J., and Taylor, K. E.: Overview of the Coupled Model Intercomparison Project Phase 6 (CMIP6) experimental design and organization, Geoscientific Model Development, 9, 1937–1958, https://doi.org/10.5194/gmd-9-1937-2016, 2016.

Fleming, E. L., Newman, P. A., Liang, Q., and Oman, L. D.: Stratospheric Temperature and Ozone Impacts of the Hunga Tonga-Hunga Ha'apai Water Vapor Injection, Journal of Geophysical Research: Atmospheres, 129, e2023JD039 298, https://doi.org/https://doi.org/10.1029/2023JD039298, e2023JD039298 2023JD039298, 2024.

Friedel, M., Chiodo, G., Sukhodolov, T., Keeble, J., Peter, T., Seeber, S., Stenke, A., Akiyoshi, H., Rozanov, E., Plummer, D., Jöckel, P., Zeng, G., Morgenstern, O., and Josse, B.: Weakening of springtime Arctic ozone depletion with climate change, Atmospheric Chemistry and Physics, 23, 10 235–10 254, https://doi.org/10.5194/acp-23-10235-2023, 2023.

Gelaro, R., McCarty, W., Suárez, M. J., Todling, R., Molod, A., Takacs, L., Randles, C. A., Darmenov, A., Bosilovich, M. G., Reichle, R., Wargan, K., Coy, L., Cullather, R., Draper, C., Akella, S., Buchard, V., Conaty, A., da Silva, A. M., Gu, W., Kim, G.-K., Koster, R., Lucchesi, R., Merkova, D., Nielsen, J. E., Partyka, G., Pawson, S., Putman, W., Rienecker, M., Schubert, S. D., Sienkiewicz, M., and Zhao, B.: The Modern-Era Retrospective Analysis for Research and Applications, Version 2 (MERRA-2), Journal of Climate, 30, 5419 – 5454, https://doi.org/10.1175/JCLI-D-16-0758.1, 2017.

Gerber, E. P. and Polvani, L. M.: Stratosphere–troposphere coupling in a relatively simple AGCM: The importance of stratospheric variability, Journal of Climate, 22, 1920–1933, 2009.

Gerber, E. P., Voronin, S., and Polvani, L. M.: Testing the Annular Mode Autocorrelation Time Scale in Simple Atmospheric General Circulation Models, Monthly Weather Review, 136, 1523 – 1536, https://doi.org/10.1175/2007MWR2211.1, 2008.

Gray, L. J., Beer, J., Geller, M., Haigh, J. D., Lockwood, M., Matthes, K., Cubasch, U., Fleitmann, D., Harrison, G., Hood, L., Luterbacher, J., Meehl, G. A., Shindell, D., van Geel, B., and White, W.: SOLAR INFLUENCES ON CLIMATE, Reviews of Geophysics, 48, https://doi.org/https://doi.org/10.1029/2009RG000282, 2010.

Hitchcock, P. and Haynes, P. H.: Stratospheric control of planetary waves, Geophysical Research Letters, 43, 11,884–11,892, https://doi.org/https://doi.org/10.1002/2016GL071372, 2016.

Jenkins, S., Smith, C., Allen, M., and Grainger, R.: Tonga eruption increases chance of temporary surface temperature anomaly above 1.5° C, Nature Climate Change, 13, 127–129, 2023.

Joshi, M. M., Charlton, A. J., and Scaife, A. A.: On the influence of stratospheric water vapor changes on the tropospheric circulation, Geophysical Research Letters, 33, https://doi.org/https://doi.org/10.1029/2006GL025983, 2006.

Jucker, M.: Are sudden stratospheric warmings generic? Insights from an idealized GCM, Journal of the Atmospheric Sciences, 73, 5061–5080, 2016.

Jucker, M.: Scaling of Eliassen-Palm flux vectors, Atmospheric Science Letters, 22, e1020, https://doi.org/https://doi.org/10.1002/asl.1020, 2021.

Jucker, M., Lucas, C., and Dutta, D.: Long-Term Climate Impacts of Large Stratospheric Water Vapor Perturbations, Journal of Climate, 37, 4507 – 4521, https://doi.org/10.1175/JCLI-D-23-0437.1, 2024.

Jörimann, A.: REMAP-GloSSAC-2023, https://doi.org/10.3929/ethz-b-000713396, 2025-01-14.

Kidston, J., Scaife, A. A., Hardiman, S. C., Mitchell, D. M., Butchart, N., Baldwin, M. P., and Gray, L. J.: Stratospheric influence on tropospheric jet streams, storm tracks and surface weather, Nature Geoscience, 8, 433–440, 2015.

Kinnison, D. E., Grant, K. E., Connell, P. S., R. D. A., and Wuebbles, D. J.: The chemical and radiative effects of the Mount Pinatubo eruption, Journal of Geophysical Research: Atmospheres, 99, 25 705–25 731, https://doi.org/https://doi.org/10.1029/94JD02318, 1994.

Kolstad, E. W., Lee, S. H., Butler, A. H., Domeisen, D. I. V., and Wulff, C. O.: Diverse Surface Signatures of Stratospheric Polar Vortex Anomalies, Journal of Geophysical Research: Atmospheres, 127, e2022JD037 422, https://doi.org/https://doi.org/10.1029/2022JD037422, e2022JD037422 2022JD037422, 2022.

Kuchar, A.: Accompanying data to "Modulation of the Northern polar vortex by the Hunga Tonga-Hunga Ha'apai eruption and associated surface response", Mendeley Data, https://doi.org/10.17632/hb3whw3nfr.1, 2025a.

Kuchar, A.: kuchaale/HTTT_SSW: First release of our code repository related to HTHH, https://doi.org/10.5281/zenodo.14743768, 2025b.

Kuchar, A., Sacha, P., Miksovsky, J., and Pisoft, P.: The 11-year solar cycle in current reanalyses: a (non)linear attribution study of the middle atmosphere, Atmospheric Chemistry and Physics, 15, 6879–6895, https://doi.org/10.5194/acp-15-6879-2015, 2015.

Marshall, L. R., Maters, E. C., Schmidt, A., Timmreck, C., Robock, A., and Toohey, M.: Volcanic effects on climate: recent advances and future avenues, Bulletin of Volcanology, 84, 54, 2022.

Martineau, P.: Reanalysis Intercomparison Dataset (RID), Japan Agency for Marine-Earth Science and Technology, https://www.jamstec.go.jp/RID/thredds/catalog/catalog.html, 2022.

Maycock, A. C., Joshi, M. M., Shine, K. P., and Scaife, A. A.: The Circulation Response to Idealized Changes in Stratospheric Water Vapor, Journal of Climate, 26, 545 – 561, https://doi.org/10.1175/JCLI-D-12-00155.1, 2013.

Millán, L., Santee, M. L., Lambert, A., Livesey, N. J., Werner, F., Schwartz, M. J., Pumphrey, H. C., Manney, G. L., Wang, Y., Su, H., Wu, L., Read, W. G., and Froidevaux, L.: The Hunga Tonga-Hunga Ha'apai Hydration of the Stratosphere, Geophysical Research Letters, 49, e2022GL099 381, https://doi.org/https://doi.org/10.1029/2022GL099381, e2022GL099381 2022GL099381, 2022.

Mitchell, D. M., Misios, S., Gray, L. J., Tourpali, K., Matthes, K., Hood, L., Schmidt, H., Chiodo, G., Thiéblemont, R., Rozanov, E., Shindell, D., and Krivolutsky, A.: Solar signals in CMIP-5 simulations: the stratospheric pathway, Quarterly Journal of the Royal Meteorological Society, 141, 2390–2403, https://doi.org/https://doi.org/10.1002/qj.2530, 2015.

Morgenstern, O., Kinnison, D. E., Mills, M., Michou, M., Horowitz, L. W., Lin, P., Deushi, M., Yoshida, K., O'Connor, F. M., Tang, Y., Abraham, N. L., Keeble, J., Dennison, F., Rozanov, E., Egorova, T., Sukhodolov, T., and Zeng, G.: Comparison of Arctic and Antarctic Stratospheric Climates in Chemistry Versus No-Chemistry Climate Models, Journal of Geophysical Research: Atmospheres, 127, e2022JD037 123, https://doi.org/https://doi.org/10.1029/2022JD037123, e2022JD037123 2022JD037123, 2022.

NASA/LARC/SD/ASDC: Global Space-based Stratospheric Aerosol Climatology Version 2.21, https://doi.org/10.5067/GLOSSAC-L3-V2.21, 2023.

Newman, P. A., Nash, E. R., and Rosenfield, J. E.: What controls the temperature of the Arctic stratosphere during the spring?, Journal of Geophysical Research: Atmospheres, 106, 19 999–20 010, https://doi.org/https://doi.org/10.1029/2000JD000061, 2001.

Newman, P. A., Lait, L. R., Kramarova, N. A., Coy, L., Frith, S. M., Oman, L. D., and Dhomse, S. S.: Record High March 2024 Arctic Total Column Ozone, Geophysical Research Letters, 51, e2024GL110 924, https://doi.org/https://doi.org/10.1029/2024GL110924, e2024GL110924 2024GL110924, 2024.

Polvani, L. M., Banerjee, A., and Schmidt, A.: Northern Hemisphere continental winter warming following the 1991 Mt. Pinatubo eruption: reconciling models and observations, Atmospheric Chemistry and Physics, 19, 6351–6366, https://doi.org/10.5194/acp-19-6351-2019, 2019.

Quaglia, I., Timmreck, C., Niemeier, U., Visioni, D., Pitari, G., Brodowsky, C., Brühl, C., Dhomse, S. S., Franke, H., Laakso, A., Mann, G. W., Rozanov, E., and Sukhodolov, T.: Interactive stratospheric aerosol models' response to different amounts and altitudes of SO_2

injection during the 1991 Pinatubo eruption, Atmospheric Chemistry and Physics, 23, 921–948, https://doi.org/10.5194/acp-23-921-2023, 2023.

Randel, W. J., Johnston, B. R., Braun, J. J., Sokolovskiy, S., Vömel, H., Podglajen, A., and Legras, B.: Stratospheric Water Vapor from the Hunga Tonga–Hunga Ha'apai Volcanic Eruption Deduced from COSMIC-2 Radio Occultation, Remote Sensing, 15, https://doi.org/10.3390/rs15082167, 2023.

Randel, W. J., Wang, X., Starr, J., Garcia, R. R., and Kinnison, D.: Long-Term Temperature Impacts of the Hunga Volcanic Eruption in the Stratosphere and Above, Geophysical Research Letters, 51, e2024GL111 500, https://doi.org/10.1029/2024GL111500, _eprint: https://onlinelibrary.wiley.com/doi/pdf/10.1029/2024GL111500, 2024.

Robock, A.: Volcanic eruptions and climate, Reviews of Geophysics, 38, 191–219, https://doi.org/https://doi.org/10.1029/1998RG000054, 2000.

Santee, M. L., Lambert, A., Froidevaux, L., Manney, G. L., Schwartz, M. J., Millán, L. F., Livesey, N. J., Read, W. G., Werner, F., and Fuller, R. A.: Strong Evidence of Heterogeneous Processing on Stratospheric Sulfate Aerosol in the Extrapolar Southern Hemisphere Following the 2022 Hunga Tonga-Hunga Ha'apai Eruption, Journal of Geophysical Research: Atmospheres, 128, e2023JD039 169, https://doi.org/https://doi.org/10.1029/2023JD039169, e2023JD039169 2023JD039169, 2023.

Sellitto, P., Podglajen, A., Belhadji, R., Boichu, M., Carboni, E., Cuesta, J., Duchamp, C., Kloss, C., Siddans, R., Bègue, N., et al.: The unexpected radiative impact of the Hunga Tonga eruption of 15th January 2022, Communications Earth & Environment, 3, 288, 2022.

Stenchikov, G., Robock, A., Ramaswamy, V., Schwarzkopf, M. D., Hamilton, K., and Ramachandran, S.: Arctic Oscillation response to the 1991 Mount Pinatubo eruption: Effects of volcanic aerosols and ozone depletion, Journal of Geophysical Research: Atmospheres, 107, ACL 28–1–ACL 28–16, https://doi.org/https://doi.org/10.1029/2002JD002090, 2002.

Stocker, M., Steiner, A. K., Ladstädter, F., Foelsche, U., and Randel, W. J.: Strong persistent cooling of the stratosphere after the Hunga eruption, Communications Earth & Environment, 5, 450, https://doi.org/https://doi.org/10.1038/s43247-024-01620-3, 2024.

Sukhodolov, T., Egorova, T., Stenke, A., Ball, W. T., Brodowsky, C., Chiodo, G., Feinberg, A., Friedel, M., Karagodin-Doyennel, A., Peter, T., Sedlacek, J., Vattioni, S., and Rozanov, E.: Atmosphere–ocean–aerosol–chemistry–climate model SOCOLv4.0: description and evaluation, Geoscientific Model Development, 14, 5525–5560, https://doi.org/10.5194/gmd-14-5525-2021, 2021.

Thompson, D. W., Baldwin, M. P., and Solomon, S.: Stratosphere–troposphere coupling in the Southern Hemisphere, Journal of the atmospheric sciences, 62, 708–715, 2005.

Vargin, P., Koval, , Guryanov, V., and Kirushov, B.: Large-scale dynamic processes during the minor and major sudden stratospheric warming events in January–February 2023, Atmospheric Research, 308, 107 545, https://doi.org/https://doi.org/10.1016/j.atmosres.2024.107545, 2024.

Veenus, V. and Das, S. S.: Observational evidence of stratospheric cooling and surface warming due to increase of stratospheric water vapor by Hunga-Tonga Hunga-Ha'apai, Research Square Preprint, https://doi.org/10.21203/rs.3.rs-3524996/v1, 2023.

Wang, X., Randel, W., Zhu, Y., Tilmes, S., Starr, J., Yu, W., Garcia, R., Toon, O. B., Park, M., Kinnison, D., Zhang, J., Bourassa, A., Rieger, L., Warnock, T., and Li, J.: Stratospheric Climate Anomalies and Ozone Loss Caused by the Hunga Tonga-Hunga Ha'apai Volcanic Eruption, Journal of Geophysical Research: Atmospheres, 128, e2023JD039 480, https://doi.org/https://doi.org/10.1029/2023JD039480, e2023JD039480 2023JD039480, 2023.

Wargan, K., Weir, B., Manney, G. L., Cohn, S. E., Knowland, K. E., Wales, P. A., and Livesey, N. J.: M2-SCREAM: A Stratospheric Composition Reanalysis of Aura MLS Data With MERRA-2 Transport, Earth and Space Science, 10, e2022EA002 632, https://doi.org/https://doi.org/10.1029/2022EA002632, e2022EA002632 2022EA002632, 2023.

Wilks, D. S.: On “Field Significance” and the False Discovery Rate, Journal of Applied Meteorology and Climatology, 45, 1181 – 1189, https://doi.org/10.1175/JAM2404.1, 2006.

Wilks, D. S.: “The Stippling Shows Statistically Significant Grid Points”: How Research Results are Routinely Overstated and Overinterpreted, and What to Do about It, Bulletin of the American Meteorological Society, 97, 2263 – 2273, https://doi.org/10.1175/BAMS-D-15-00267.1, 2016.

Wilmouth, D. M., Østerstrøm, F. F., Smith, J. B., Anderson, J. G., and Salawitch, R. J.: Impact of the Hunga Tonga volcanic eruption on stratospheric composition, Proceedings of the National Academy of Sciences, 120, e2301994 120, https://doi.org/10.1073/pnas.2301994120, 2023.

Xu, J., Li, D., Bai, Z., Tao, M., and Bian, J.: Large Amounts of Water Vapor Were Injected into the Stratosphere by the Hunga Tonga–Hunga Ha’apai Volcano Eruption, Atmosphere, 13, https://doi.org/10.3390/atmos13060912, 2022.

Yu, W., Garcia, R., Yue, J., Smith, A., Wang, X., Randel, W., Qiao, Z., Zhu, Y., Harvey, V. L., Tilmes, S., and Mlynczak, M.: Mesospheric Temperature and Circulation Response to the Hunga Tonga-Hunga-Ha’apai Volcanic Eruption, Journal of Geophysical Research: Atmospheres, 128, e2023JD039 636, https://doi.org/https://doi.org/10.1029/2023JD039636, e2023JD039636 2023JD039636, 2023.

Zhang, J., Kinnison, D., Zhu, Y., Wang, X., Tilmes, S., Dube, K., and Randel, W.: Chemistry Contribution to Stratospheric Ozone Depletion After the Unprecedented Water-Rich Hunga Tonga Eruption, Geophysical Research Letters, 51, e2023GL105 762, https://doi.org/https://doi.org/10.1029/2023GL105762, e2023GL105762 2023GL105762, 2024a.

Zhang, J., Wang, P., Kinnison, D. E., Solomon, S., Guan, J., and Zhu, Y.: Stratospheric chlorine processing after the unprecedented Hunga Tonga eruption, Authorea Preprints, 2024b.

Zhou, X., Dhomse, S. S., Feng, W., Mann, G., Heddell, S., Pumphrey, H., Kerridge, B. J., Latter, B., Siddans, R., Ventress, L., Querel, R., Smale, P., Asher, E., Hall, E. G., Bekki, S., and Chipperfield, M. P.: Antarctic Vortex Dehydration in 2023 as a Substantial Removal Pathway for Hunga Tonga-Hunga Ha’apai Water Vapor, Geophysical Research Letters, 51, e2023GL107 630, https://doi.org/https://doi.org/10.1029/2023GL107630, e2023GL107630 2023GL107630, 2024.

Zhu, Y., Akiyoshi, H., Aquila, V., Asher, E., Bednarz, E. M., Bekki, S., Brühl, C., Butler, A. H., Case, P., Chabrillat, S., Chiodo, G., Clyne, M., Falletti, L., Colarco, P. R., Fleming, E., Jörimann, A., Kovilakam, M., Koren, G., Kuchar, A., Lebas, N., Liang, Q., Liu, C.-C., Mann, G., Manyin, M., Marchand, M., Morgenstern, O., Newman, P., Oman, L. D., Østerstrøm, F. F., Peng, Y., Plummer, D., Quaglia, I., Randel, W., Rémy, S., Sekiya, T., Steenrod, S., Sukhodolov, T., Tilmes, S., Tsigaridis, K., Ueyama, R., Visioni, D., Wang, X., Watanabe, S., Yamashita, Y., Yu, P., Yu, W., Zhang, J., and Zhuo, Z.: Hunga Tonga-Hunga Ha’apai Volcano Impact Model Observation Comparison (HTHH-MOC) Project: Experiment Protocol and Model Descriptions, EGUsphere, 2024, 1–32, https://doi.org/10.5194/egusphere-2024-3412, 2024.